www.dergipark.gov.tr
ISSN:2148-3736
El-Cezerî Fen ve Mühendislik Dergisi
Cilt: 9, No: 2, 2022 (777-787)

El-Cezerî Journal of Science and Engineering
Vol: 9, No: 2, 2022 (777-787)
DOI : 10.31202/ecjse.1008121

ECJSE

Research Paper / Makale

Modulated Model Predictive Torque Control for Interior Permanent Magnet Synchronous Machines

Uğur Ufuk KÖRPE[1a], Mustafa GÖKDAĞ[2c], Mikail KOÇ[1b], Ozan GÜLBÜDAK[2d]

[1]Kirsehir Ahi Evran University, Engineering and Architecture Faculty, Electrical and Electronics Engineering Department, Kırşehir/ Türkiye,
[2]Karabuk University, Engineering Faculty, Electrical and Electronics Engineering Department, Karabük/Türkiye
ugur.korpe@ahievran.edu.tr

Received/Geliş: 11.10.2021 **Accepted/Kabul:** 14.12.2021

Abstract: Thanks to the advancements in the processor industry, the popularity in the industrial applications of Finite control set model predictive control (FCS-MPC) is increasing. FCS-MPC has several advantages, such as high closed-loop bandwidth, the inclusion of the control constraints, and nonlinearities. However, the control signals are directly produced by the predictive controller since no modulator is used. Hence, the system has non-fixed switching frequency, and the maximum achievable switching frequency is limited by the half of the sampling frequency. However, the control goals may suffer from the undesired ripples in case of a noticeable low switching frequency. To eliminate these ripples the sampling period of the system can be reduced. But this increases the computational burden on the processor. To overcome the unwanted oscillations in the control variables and decrease the computational burden on the processor, a modulated model predictive control (M^2PC) strategy is proposed in this paper. The M^2PC combines the space vector pulse width modulator (SVPWM) and FCS-MPC. Torque of the interior permanent magnet synchronous motor (IPMSM) is controlled with M^2PC method. The motor is controlled in a constant torque region with the combination of the M^2PC method and maximum torque per ampere (MTPA) control strategy. The comparative results of the conventional MPC method and M^2PC method are reported in the paper and the superiority of the M^2PC strategy is validated by simulation works. The results demonstrate that the M^2PC method significantly reduces total harmonic distortion (THD) in stator currents. Based on the results, the M^2PC method provides a better control performance for IPMSMs with significantly reduced torque ripples.

Keywords: Modulated Model Predictive Control, Model Predictive Control, IPMSM

Gömülü Mıknatıslı Senkron Motorların Modüleli Model Öngörülü Tork Kontrolü

Öz: İşlemci endüstrisindeki ilerlemeler sayesinde Model Öngörülü Kontrol'ün endüstriyel uygulamalarındaki popülaritesi artmaktadır. MÖK'ün yüksek kapalı döngü bant genişliğine sahip olması, kontrol kısıtlamalarının ve doğrusal olmayan durumların kontrole dâhil edilmesi gibi birçok avantajı bulunmaktadır. Fakat modülatör kullanılmadığı için kontrol sinyalleri doğrudan öngörücü kontrolör tarafından üretilmektedir. Bundan dolayı sistem değişken anahtarlama frekansına sahiptir ve maksimum elde edilebilecek frekans örnekleme frekansının yarısı ile sınırlıdır. Bununla birlikte, düşük anahtarlama frekanslarında kontrol değişkenlerinde istenmeyen dalgalanmalar oluşmaktadır. Bu dalgalanmaları elimine etmek için sistemin örnekleme periyodu düşürülebilir. Ama bu işlemcinin üzerindeki matematiksel yükü arttırmaktadır. Kontrol değişkenlerindeki istenmeyen dalgalanmaları azaltmak ve işlemcinin üzerindeki matematiksel yükü hafifletmek için bu çalışmada Modüleli Model Öngörülü Kontrol (MMÖK) stratejisi önerilmiştir. MMÖK metodu MÖK metodu ile uzay vektör darbe genişlik modülasyonun (UVDGM) birleşimidir. Gömülü mıknatıslı senkron motorun (GMSM) torku MMÖK metodu ile kontrol edilmiştir. Motor, MMÖK metodu ve akım başına maksimum tork (ABMT) kontrol stratejisinin birleşimiyle sabit tork bölgesinde kontrol edilmiştir. Çalışmada geleneksel MÖK metodu ile MMÖK metodunun sonuçları karşılaştırılmış ve MMÖK kontrol stratejisinin üstünlüğü simülasyon çalışmaları

How to cite this article
Körpe U.U, Gökdağ, M. Koç, M. Gülbüdak, O., "Modulated Model Predictive Torque Control for Interior Permanent Magnet Synchronous Machines" El-Cezerî Journal of Science and Engineering, 2022, 8 (2); 777-787.

Bu makaleye atıf yapmak için
Körpe U.U, Gökdağ, M. Koç, M. Gülbüdak, O., "Gömülü Mıknatıslı Senkron Motorların Modüleli Model Öngörülü Tork Kontrolü" El-Cezerî Journal of Science and Engineering, 2022, 9 (2); 777-787.
ORCID : [a]0000-0001-6450-1697, [b]0000-0001-5589-2278, [c]0000-0003-1465-1878, [d]0000-0001-9517-3630

ile doğrulanmıştır. Sonuçlar, MMÖK yönteminin stator akımlarındaki toplam harmonik bozulmayı (THB) önemli ölçüde azalttığını göstermektedir. MMÖK yönteminin torkdaki dalgalanmaları önemli ölçüde azaltarak, GMSM ler için daha iyi kontrol performansı sağladığı simülasyon sonuçları ile doğrulanmıştır.

Anahtar Kelimeler: Model Öngörülü Kontrol, Modüleli Model Öngörülü Kontrol, GMSM

1. Introduction

The interest in electric vehicle technology is increasing as they use renewable energy sources and thus reduce carbon dioxide emission [1, 2]. The use of permanent magnet synchronous motors (PMSM) in electric vehicle applications is increasing day by day due to their advantages such as high efficiency, low rotor losses, high torque-power ratio, and no-slip compared to ac induction motors [3]. PMSMs can be classified into two groups in terms of the placement of the permanent magnet in the rotor: 1) IPMSM 2) SPMSM. In surface-mounted PMSMs, the permanent magnet is on the rotor surface while in interior PMSMs, the permanent magnet is embedded inside of the rotor [4]. Based on the placement of the magnets in the rotor, the torque is generated by the magnetizing flux in SPMSMs. The magnet placement in IPMSMs causes reluctance to change as the motor rotates. This reluctance change is called saliency. This saliency introduces another torque term which is called reluctance torque in IPMSMs, unlike SPMSMs. In IPMSMs, the torque is generated by both the magnetizing flux and reluctance torque. Hence, the total torque in IPMSMs compared to SPMSMs increases by exploiting the reluctance torque.

Commonly used torque control techniques for PMSMs are the field-oriented control (FOC) and direct torque control (DTC). Besides these conventional torque control methods, the popularity of the FCS-MPC method has been increasing because of the advantages of this control strategy. This control method aims to obtain the optimum voltage vector to be applied to the inverter. The motor stator current is predicted for all admissible voltage vectors by using the discrete-time mathematical model of the system. The predicted stator current and the corresponding reference term are introduced in the cost function to calculate the error term. Then, the optimum vector that reduces the cost is applied to the system [5]. The major benefits of the FCS-MPC strategy are the ease of including the operation constraints, fast transient response, and the control of the multiple control goals [6]. Despite the advantages of the FCS-MPC, the control system has a non-fixed switching frequency. Because the formation of the closed-loop system does not contain the linear modulator (or other advanced modulator schemes), thus the unregulated switching frequency is inevitable. The critical problem with the uncontrolled switching frequency is that the mechanical torque and stator current are deteriorated. Distorted current waveforms increase the undesired torque ripples during steady-state operation. To alleviate the ripples, the sampling period of the discrete controller can be reduced. Although the choice of a lower sampling period alleviates the high ripple problem, it incurs the high computational burden [7]. There is a practical limit on the sampling frequency of microprocessor for the real-time implementation. In particular, to lower the sampling period is impractical where a high amount of control calculations need to be performed. The favorable solution to reduce the torque and stator current ripples without reducing sampling time is using a modulator. The main idea of including the modulator is that multiple active vectors can be used to get the control variable closer to the associated references. Therefore, the trajectory tracking performance is improved, and unwanted ripples are vanquished. The predictive control method combined with SVPWM is called modulated model predictive control [8]. The M^2PC method provides better steady-state performance with no regard for the prediction step.

The discussed control method can be adopted to control the IPMSMs in both constant torque and constant power regions [9]. The purpose of the MTPA control technique is to obtain the operating point where the stator current magnitude is minimum to produce the desired torque value [9]. The torque control of SPMSM with MTPA is realized with the control of the magnetizing current, with q-axis current control since there is no saliency in these motors. However, the torque control of IPMSM with MTPA is realized with the control of both the magnetizing torque and reluctance torque because of the saliency.

In the literature, the conventional MPC method is widely used in chemical industries at first because of the long time constants. In most cases, the process is slow, and the computational burden is not problematic. However, the scenario is completely different in the power electronics application where the sampling frequency varies between 10μs - 100μs. Different types of converters and machines are controlled with the conventional MPC and M^2PC methods due to advancements in the processor industry [10-14]. The current control of three phase two level voltage-source inverter with MPC and M^2PC method is performed, and the results are compared with each other [15, 16]. According to simulation results reported in [15], THD values of the stator current are reduced by applying the M^2PC method. The benefit of the regulated switching frequency is demonstrated by performing the M^2PC method. The control of PMSM with MPC and M^2PC method is performed with different types of inverter topologies and the results are compared with each other [17-19]. PMSM is driven by three phase two level voltage-source inverter in [17, 18] and in [19], PMSM is driven by three level NPC inverter. The simulation results show that M^2PC method gives better control performance than conventional MPC method and reduces THD in stator currents and ripple in electromagnetic torque significantly. However, in [15], [17-19], simulations for both methods are performed for only one switching frequency value. In [17-19], no assessment work has been conducted to evaluate the closed-loop performance and stator current THD. Furthermore, the dynamic performance of the MPC and M^2PC under torque variations has not been comprehensively investigated. Because the motor controlled in [17-19] is SPMSM, there is no information about control performance of IPMSM with conventional MPC and M^2PC methods.

In this paper, torque control of IPMSM is performed with M^2PC method. The simulation-based comparison results between M^2PC and the conventional MPC are reported in terms of electromagnetic torque variations and THD in stator current. The simulation results show that the M2PC method improves steady-state performance of the control system with decreasing THD in stator currents and ripple in electromagnetic torque. The other important advantage of the M^2PC method is to perform the control algorithm at higher sampling times and decreases the computational burden of the processor.

2. System Model

2.1. Inverter

The circuit diagram of an inverter fed IPMSM is shown in Figure 1. The three phase two level voltage-source inverter (VSI) has eight switching states. Among these eight voltage vectors, two of them are zero switching states and the other six are active switching states. An ideal inverter is employed in the simulated drives and the inverter is assumed to be in a balanced load state [20].

$$\begin{bmatrix} V_{An} \\ V_{Bn} \\ V_{Cn} \end{bmatrix} = \frac{V_{DC}}{3} \begin{bmatrix} 2 & -1 & -1 \\ -1 & 2 & -1 \\ -1 & -1 & 2 \end{bmatrix} \begin{bmatrix} S_1 \\ S_3 \\ S_5 \end{bmatrix} \tag{1}$$

where V_{An}, V_{Bn}, V_{Cn} are A, B, C phase to neutral voltages, respectively, V_{DC} refers to DC bus voltage, and S_1, S_3, S_5 are the high-side switches of inverter phase a, b, c, respectively.

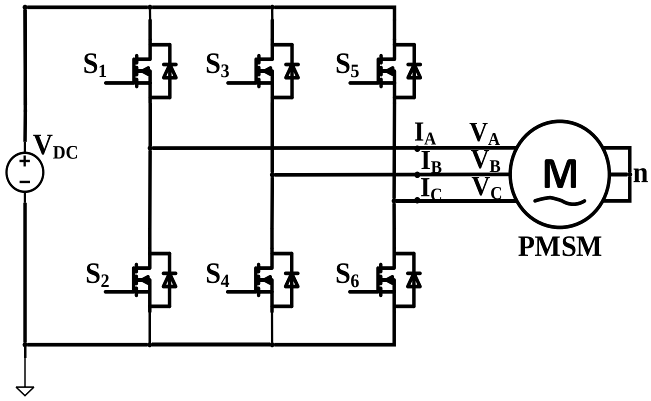

Figure 1. Voltage source inverter (VSI) topology

2.2. IPMSM Mathematical Model

In this study, the mathematical model of the IPMSM is given in the d-q axes reference frame where d-q axes rotate at the synchronous speed. The dynamic model of the IPMSM is given by

$$V_d = RI_d + L_d \frac{dI_d}{dt} - \omega_e L_q I_q \tag{2}$$

$$V_q = RI_q + L_q \frac{dI_q}{dt} + \omega_e (L_d I_d + \varphi_m) \tag{3}$$

where $V_{d\text{-}q}$ is d-q axes voltage, $I_{d\text{-}q}$ are d-q axes currents, $L_{d\text{-}q}$ are d-q axes inductances, R is stator resistance, ω_e is synchronous speed, φ_m is permanent magnet flux linkage. Electromagnetic torque expression is shown in equation (4), where T_e is electromagnetic torque and p denotes the number of pole pairs. The electromagnetic torque equation consists of two parts. The first part is the torque produced by the permanent-magnet and the second part is reluctance torque caused by the saliency.

$$T_e = \frac{3p}{2}(\varphi_m I_q - I_d I_q (L_q - L_d)) \tag{4}$$

Rotor electrical angle of the motor can be found using equation (5) where θ_e denotes the rotor electrical angle.

$$\theta_e(t) = \int \omega_e(t)\, dt \tag{5}$$

In M^2PC and MPC methods, control of the system can be done by expressing motor dynamic equations in discrete time. The discrete-time versions of (2)-(3) can be obtained by applying the Forward Euler (FE) method as in (6).

$$\frac{df}{dt} = \frac{f(k+1) - f(k)}{T_s} \tag{6}$$

where T_S is sampling time. The discrete-time d-q axes stator currents are defined in **Hata! Başvuru kaynağı bulunamadı.**)-(7).

$$I_d(k+1) = \frac{V_d(k) T_S}{L_d} + \frac{\omega_e L_q I_q(k) T_S}{L_d} + I_d(k)\left(1 - \left(\frac{RT_S}{L_d}\right)\right) \tag{7}$$

$$I_q(k+1) = \frac{V_q(k)T_s}{L_q} - \frac{\omega_e L_d I_d(k)T_s}{L_q} - \frac{\omega_e \varphi_m T_s}{L_q} + I_q(k)\left(1-\left(\frac{RT_s}{L_q}\right)\right) \quad (7)$$

By applying Forward-Euler discretization to (5) and shifting the variables one step back, the discrete-time expression for rotor electrical angle is obtained as in (8).

$$\theta_e(k) = \theta_e(k-1) + \omega_e(k-1)T_s \quad (8)$$

3. Proposed Method

3.1.Model Predictive Control (MPC)

The block diagram of the conventional MPC method is shown in Figure 2. This control method aims to find the optimum voltage vector to be applied to the VSI. To find this voltage vector first the mechanical speed, ω_m, is measured via a sensor. The measured stator currents in the a-b-c frame are converted into d-q axes reference frame. In the algorithm, all phase to neutral voltages of the VSI is calculated by substituting voltage vectors in (1), and these phase to neutral voltages are transformed to d-q axes frame.

$$V_d = \frac{2}{3}\left(V_{An}\cos\theta_e + V_{Bn}\cos\left(\theta_e - \frac{2\pi}{3}\right) + V_{Cn}\cos\left(\theta_e + \frac{2\pi}{3}\right)\right) \quad (9)$$

$$V_q = \frac{2}{3}\left(-V_{An}\,sin\,\theta_e - V_{Bn}\,sin\left(\theta_e - \frac{2\pi}{3}\right) - V_{Cn}\,sin\left(\theta_e + \frac{2\pi}{3}\right)\right) \quad (10)$$

Then, the determined phase-to-neutral voltages are used to predict the future values of the d-q axis currents based on **Hata! Başvuru kaynağı bulunamadı.**) and (7). There are totally eight current predictions for eight switching vectors.

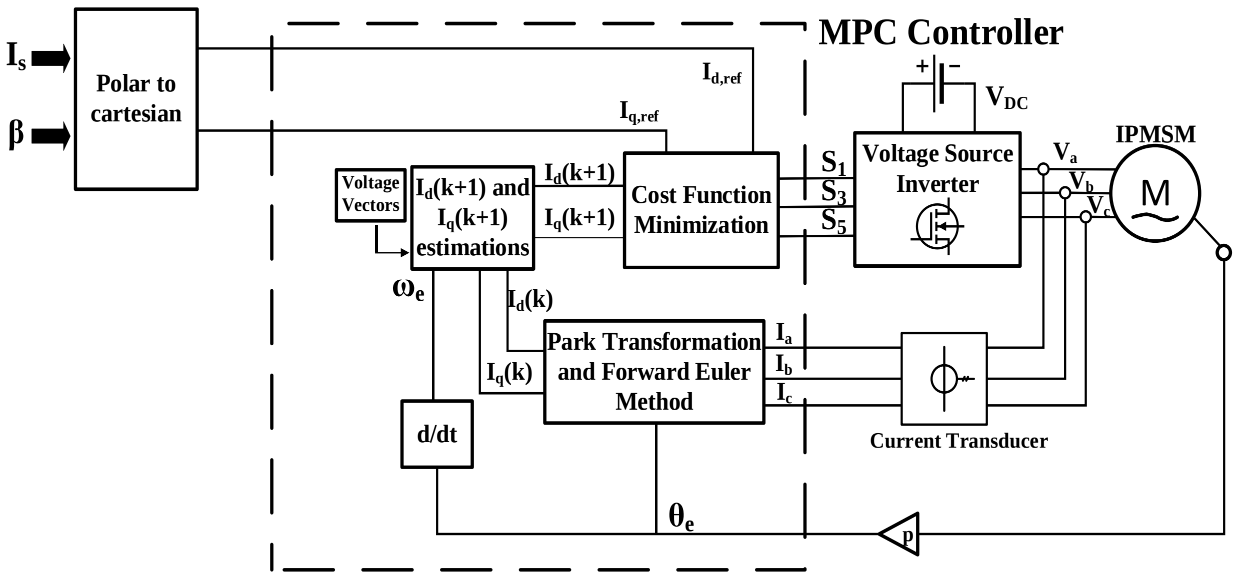

Figure 2. Conventional MPC block diagram

$$G = (I_{d,ref} - I_d(k+1))^2 + (I_{q,ref} - I_q(k+1))^2 \quad (11)$$

The vector that minimizes (11) is chosen for the next time interval. Where G in (12) is the objective function of the conventional MPC method. The application of the gate signals is directly performed by the controller [5]. This approach is called the conventional MPC method as illustrated in Figure 2.

3.2. Modulated Model Predictive Control (M^2PC)

To improve the steady-state performance of the system, the M^2PC method, which combines SVPWM and FCS-MPC method, is proposed. The block diagram of the M^2PC method is shown in Figure 3. As in the typical SVPWM technique, the optimum voltage vector is obtained by using two active voltage vectors and zero voltage vectors. By modulating between these two active and zero voltage vectors, the average current error becomes zero [18]. To find the optimum active and zero vectors, the cost function values of every voltage vector according to equation (11) are stored. Duty cycles of active vectors and zero vectors in each sector can be found according to equations (12)-(14) by using stored cost functions [15].

$$d_0 = \frac{T_s G_1 G_2}{G_0 G_1 + G_1 G_2 + G_0 G_2} \tag{12}$$

$$d_1 = \frac{T_s G_0 G_2}{G_0 G_1 + G_1 G_2 + G_0 G_2} \tag{13}$$

$$d_2 = \frac{T_s G_0 G_1}{G_0 G_1 + G_1 G_2 + G_0 G_2} \tag{14}$$

where $d_{0\text{-}1\text{-}2}$ are the duty cycles of zero and two active voltage vectors, respectively. $G_{0\text{-}1\text{-}2}$ are the cost functions values of every voltage vector in every sector that are stored to determine the active voltage vectors and zero voltage vector, respectively. To enable the use of the M^2PC, the objective function in (12) is modified.

$$g = d_0 G_0 + d_1 G_1 + d_2 G_2 \tag{15}$$

where g is the reformulated objective function of the M^2PC method.

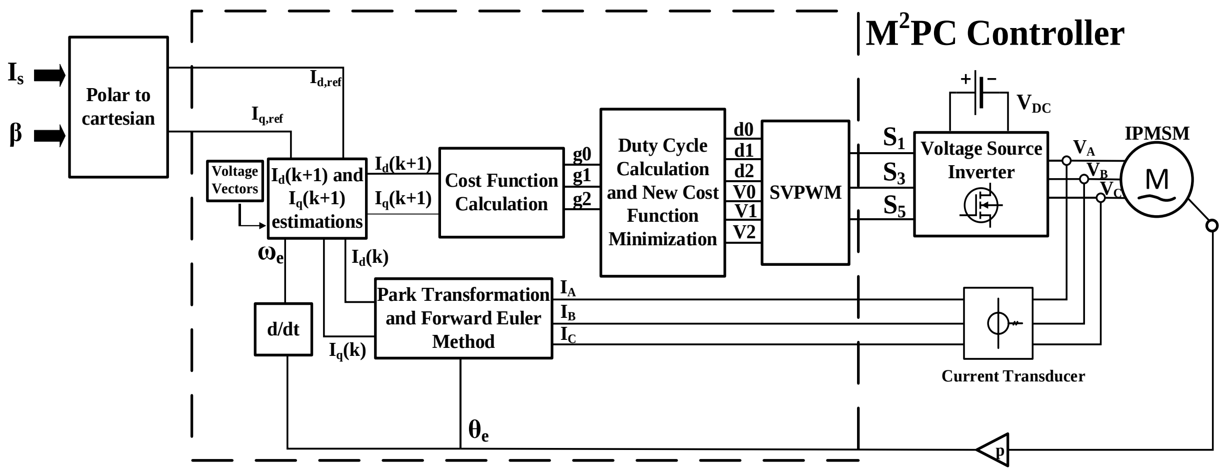

Figure 3. Block diagram of the M^2PC method

The two active voltage vectors and zero vector that minimizes (15) are selected and applied to the inverter [13]. Hence, the fixed switching frequency is achieved. The modulator uses these voltage vectors and the duty cycle values to generate gate pulses.

3.3. Operation in Constant Torque Region

In SPMSMs, since L_d=L_q, the torque can be controlled by utilizing q-axis current according to (4). Unlike SPMSM, since $L_d \neq L_q$ in IPMSMs, the d-axis current must also be controlled, beside the q-axis current. Stator current vector (I_s), d-q axes current vectors (I_d, I_q), stator (φ_s) and magnetizing flux vectors (φ_m), and stator voltage vector (V_s) are shown in Figure 4 for the stationary and rotating synchronous frames. According to Figure 4, the β angle is the angle between the stator current vector and q-axis current vector. The stator current achieves its maximum value when β equals 0°. On the other hand, the maximum reluctance torque is obtained in the case of β=45°. Therefore, the optimum value of β is within the range of 0-45° to get benefit from reluctance torque and magnetizing torque. Further details regarding how to obtain optimum beta angle is discussed in [21].

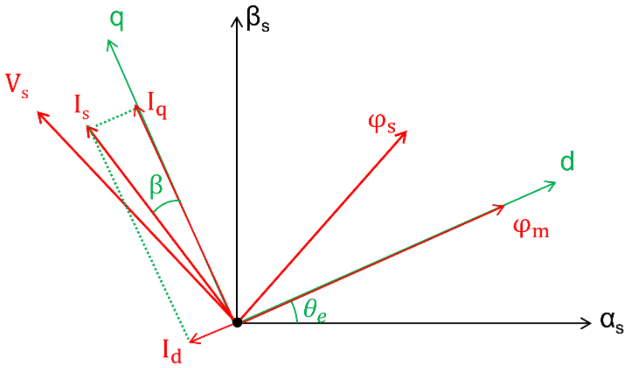

Figure 4. Current, voltage and flux vectors illustration in the α_s-β_s frame

4. Results

The M²PC method is tested by simulation work. The proposed method and the conventional method are compared at different evaluation metrics. The motor and simulation parameters are listed in

Table 1.

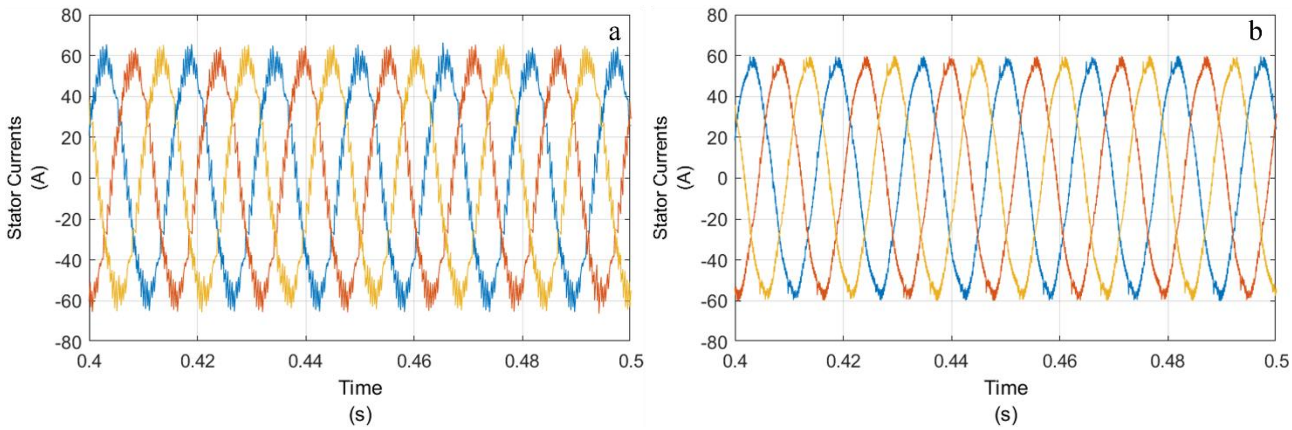

Figure 5. Stator Currents waveforms at ω_m = 100 rad/s and T_e = 10 Nm; (a) Conventional MPC method, (b) The M^{2}PC method

The comparative simulation results are shown in Figure 5 - 7 at the mechanical speed of the motor is ω_m=100 rad/s, and the applied torque is T_e=10Nm. The stator current waveforms of conventional MPC and the M^{2}PC method are shown in Figure 5. According to Figure 5, the stator current is less distorted for the M^{2}PC method. The electromagnetic torque of the motor is shown in Figure 6 for conventional MPC and the M^{2}PC method. As can be seen, the torque ripple is lower for the M^{2}PC method than conventional MPC. A-B phase-to-phase voltage waveforms are shown in Figure 7. The comparison results in terms of THD in stator currents are reported in **Figure 8**. The THD value in stator current for the conventional MPC is 11.58% for a sampling period of 100 µs. On the other hand, the THD value in stator current for the M^2PC is 5.87% for the same sampling period which corresponds to a 10 kHz switching frequency value. The simulation results prove that the M^2PC method reduces the THD value by nearly 50% when the system is controlled with M^2PC method.

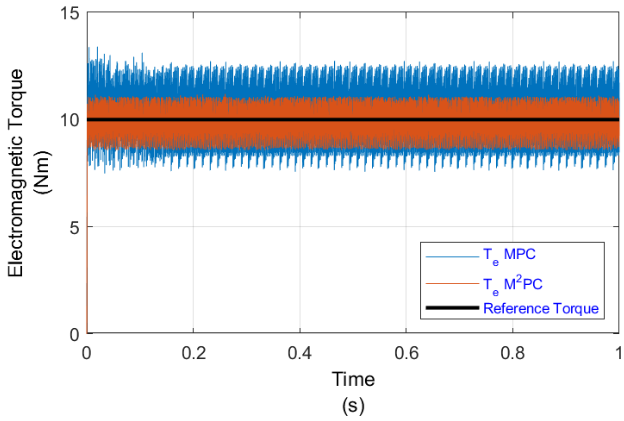

Figure 6. Electromagnetic torque waveforms at $\boldsymbol{\omega}_m$ = 100 rad/s and T_e = 10 Nm

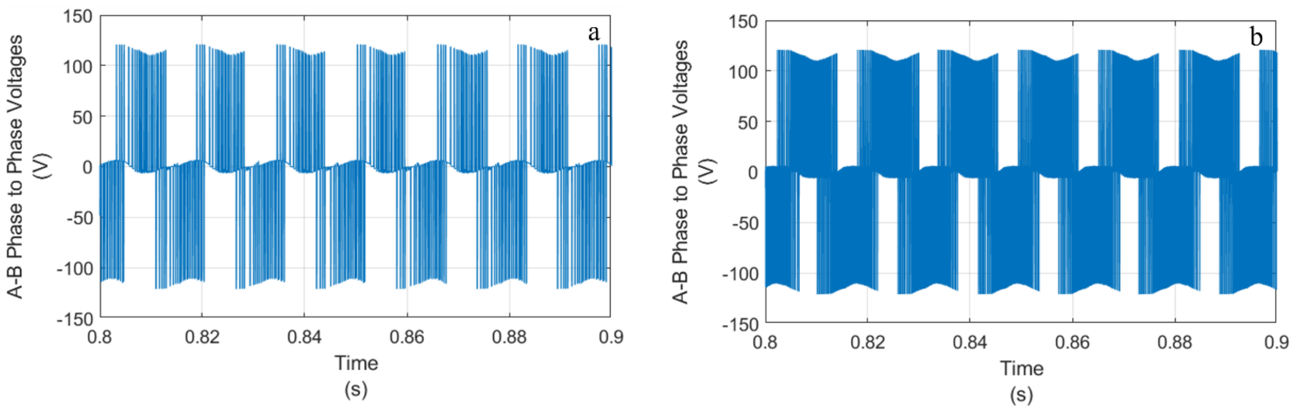

Figure 7. Inverter A-B phase to phase voltage waveforms at $\boldsymbol{\omega}_m$ = 100 rad/s and T_e = 10 Nm; (a) Conventional MPC method, (b) The M^2PC method

Table 1. Motor and Simulation Parameters

Parameter	Description	Values
T_S	Sampling Time	100 µs
Φ	Number of pole pairs	4
P	Continuous power	4.1 kW
T	Continuous torque	15.7 Nm
ω_m (rpm)	Nominal speed	2500 rpm
L_d	d-axis Inductance	0.282 mH
L_q	q-axis Inductance	0.827 mH
φ_m	PM Flux Linkage	0.0182 Wb
R	Phase Resistance	0.0463 Ω

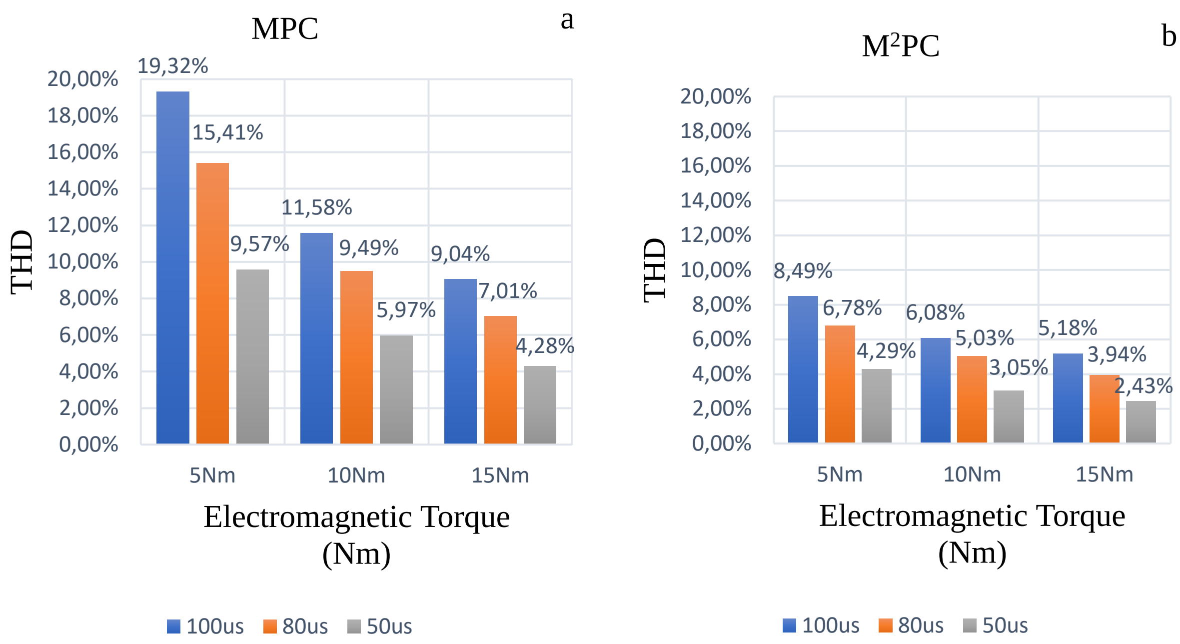

Figure 8. THD values at different sampling times and for different electromagnetic torque values; (a) Conventional MPC method, (b) The M^2PC method

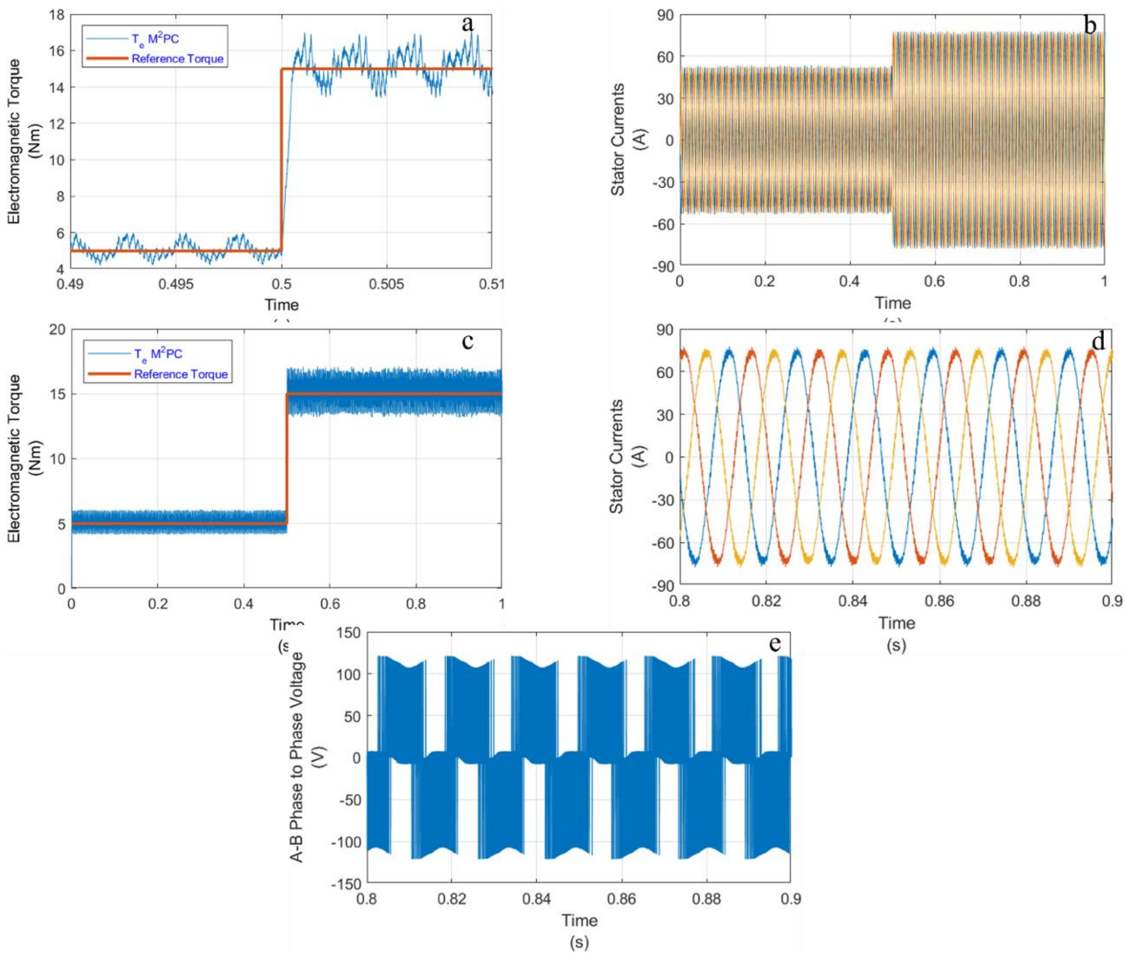

Figure 9. Waveforms of the load side at $\boldsymbol{\omega}_m$ = 100 rad/s and T_e = 5 Nm and T_e = 15 Nm; (a) Electromagnetic torque, (b) Stator currents, (c) Transient response of electromagnetic torque, (d) Zoom-in stator currents, (e) Inverter A-B phase to phase voltages

To examine the torque response of the M^2PC method, the torque step is applied at t=0.5s to the closed-loop system. Figure 9 presents the dynamic response of the M^2PC control method. In this scenario, ω_m=100 rad/s which is the mechanical speed of the motor, the torque profile T_e=5 Nm between t=0-0.5 s and T_e=15 Nm between t=0.5-1 s. The sampling time is T_S=100 µs. During the torque transition, the magnitude of the stator current is adjusted by M^2PC method to satisfy the new torque command. The motor is producing electromagnetic torque once the new torque command is applied at t=0.5 s. As a result, the M^2PC method provides a better result at wide operating points compared to the conventional MPC method.

5. Conclusions

This paper compares the conventional MPC and M^2PC control strategies for IPMSM. SVPWM technique and FCS-MPC technique are combined to achieve better steady-state performance at fixed switching frequency. The simulation results show the THD in stator currents and electromagnetic torque ripple are significantly reduced in M^2PC method compared to the conventional MPC method at different sampling times and at different electromagnetic torque points. Simulation results at different sampling times show that the sampling time of the system must be reduced for conventional MPC method so that the THD in stator currents approaches the results obtained with M^2PC method but computational burden on the processor increases drastically at low sampling times. The proposed M^2PC method performs very well for high sampling times and hence, computational burden on the processor reduces. From the results obtained at different sampling times and for different electromagnetic torque values show torque control of IPMSM with M^2PC method can be performed at desired sampling times and desired electromagnetic torque values. As a result, the M^2PC method provides a better system performance than the conventional MPC method over a wide range.

Acknowledgments

This study has been supported by the Scientific and Technological Research Council of Turkey (TUBITAK) through the Scientific and Technological Research Projects Funding Program (1001) with a project numbered as 118E858.

Authors' contributions

The authors contributed equally to the study.

Competing interests

The authors declare that they have no competing interests.

References

[1]. Halim M.F.M.A., Sulaiman E., ´´Permanent Magnet Flux Switching Torque Performance Indicator,´´ El Cezeri, 2021, 8 (2) : 582-591.

[2]. Bayraktar M., Yıldırız E., ´´Constant Current/Voltage Charging of A 250W E-Bike with Wireless Power Transfer,´´ El Cezeri, 2020, 7 (1) : 189-197.

[3]. Kıyak I., Kaya K.Y., ´´Elektrikli Taşıtlarda Kullanılan İndüksiyon / Sabit Mıknatıslı Motor Sürücülerinin Simülasyonu ve Motor Dinamiklerinin Analizi,´´ Int. J. Adv. Eng. Pure Sci., 2020, 32 (2) : 152-157.

[4]. Murakami H., Honda Y., Kiriyama H., Morimoto S., Takeda Y., ´´The performance comparison of SPMSM, IPMSM and SynRM in use as air-conditioning compressor,´´ Conference Record of the 1999 IEEE Industry Applications Conference. Thirty-Forth IAS Annual Meeting (Cat. No.99CH36370), Phoenix, USA, 840-845, 1999.

[5]. Wang F., Mei X., Rodriguez J., Kennel R., ´´Model predictive control for electrical drive systems-an overview,´´ CES Trans. Electr. Mach. Syst., 2017, 1(3) : 219-230.

[6]. Elmorshedy M.F., Xu W., El-Sousy F.F.M., Islam M.R., Ahmed A.A., ´´Recent Achievements in Model Predictive Control Techniques for Industrial Motor: A Comprehensive State-of-the-Art,´´ IEEE Access, 2021, 9 : 58170-58191.
[7]. Vazquez S., Rodriguez J., Rivera M., Franquelo L.G., Norambuena M., ´´Model Predictive Control for Power Converters and Drives: Advances and Trends,´´ IEEE Trans. Ind. Electron., 2017, 64(2) : 935-947.
[8]. Yaramasu V., Milev K., Dekka A., Rivera M., Rodriguez J., Rojas F., ´´Modulated Model Predictive Current Control of a Four-Leg Inverter,´´ 2020 11th Power Electronics, Drive Systems, and Technologies Conference (PEDSTC), Tehran, Iran, 1-6, 2020.
[9]. Li K., Wang Y., ´´Maximum Torque Per Ampere (MTPA) Control for IPMSM Drives Based on a Variable-Equivalent-Parameter MTPA Control Law,´´ IEEE Trans. Power Electron., 2018, 34(7) : 7092-7102.
[10]. Gulbudak O., Gokdag M., ´´FPGA-Based Model Predictive Control for Power Converters,´´ 2020 2nd Global Power, Energy and Communication Conference (GPECOM), Izmir, Turkey, 30-35, 2020.
[11]. Vijayagopal M., Zanchetta P., Empringham L., de Lillo L., Tarisciotti L., Wheeler P., ´´Control of a Direct Matrix Converter With Modulated Model-Predictive Control,´´ IEEE Trans. Ind. Appl., 2017, 53(3) : 2342-2349.
[12]. Xiao D., Alam K.S., Norambuena M., Rahman M.F., Rodriguez J., ´´Modified Modulated Model Predictive Control Strategy for a Grid-Connected Converter,´´ IEEE Trans. Ind. Appl., 2021, 68(1) : 575-585.
[13]. Milev K., Yaramasu V., Dekka A., Kouro S., ´´Modulated Predictive Current Control of PMSG-Based Wind Energy Systems,´´ 2020 11th Power Electronics, Drive Systems, and Technologies Conference (PEDSTC), Tehran, Iran, 1-6, 2020.
[14]. Gokdag M., Gulbudak O., ´´Imposed Source Current Predictive Control for Battery Charger Applications with Active Damping,´´ Sak. Univ. J. Sci., 2019, 23(5) : 964-971.
[15]. Rivera M., Morales F., Baier C., Muñoz J., Tarisciotti L., Zanchetta P., Wheeler P., ´´A modulated model predictive control scheme for a two-level voltage source inverter,´´ 2015 IEEE Inter. Conference on Industrial Technology (ICIT), Seville, Spain, 2224-2229, 2015.
[16]. Zeng J., Lin Q., Chen S., Su X., Lin X., Chen T., ´´A Modulated Model Predictive Control for Three Phase Voltage Source Inverter,´´ 2020 Chinese Automation Congress (CAC), Shanghai, China, 2899-2902, 2020.
[17]. Zhang F., Peng T., Dan H., Lin J., Su M., ´´Modulated model predictive control of permanent magnet synchronous motor,´´ 2018 IEEE International Conference on Industrial Electronics for Sustainable Energy Systems (IESES), Hamilton, New Zealand, 130-133, 2018.
[18]. Garcia C., Rodriguez J., Odhano S., Zanchetta P., Davari S.A., ´´Modulated Model Predictive Speed Control for PMSM Drives,´´ 2018 IEEE Int. Conf. Electr. Syst. Aircraft, Railw. Sh. Propuls., Nottingham, UK, 1-6, 2018.
[19]. Wang Q., Rivera M., Riveros J.A., Wheeler P., ´´Modulated Model Predictive Current Control for PMSM Operating With Three-level NPC Inverter,´´ 2019 IEEE 15th Brazilian Power Electron. Conf. 5th IEEE South. Power Electron. Conf. COBEP/SPEC 2019, Santos, Brazil, 1-5, 2019.
[20]. Rodriguez J., Pontt J., Silva C.A., Correa P., Lezana P., Cortes P., Ammann U., ´´Predictive Current Control of a Voltage Source Inverter,´´ IEEE Trans. Ind. Electron., 2007, 54(1): 495-503.
[21]. Koç M., Emiroğlu S., Tamyürek B., ´´Analysis and simulation of efficiency optimized IPM drives in constant torque region with reduced computational burden,´´ Turkish J. Electr. Eng. Comput. Sci., 2021, 29(3) : 1643-1658.